

Original Article

Cite this article: Fang, K., Wen, B., Liu, L., Han, S., & Zhang, W. (2025). Disrupted intersubject variability architecture in structural and functional brain connectomes in major depressive disorder. *Psychological Medicine*, 55, e56, 1–12

<https://doi.org/10.1017/S0033291725000078>

Received: 04 December 2024

Revised: 06 January 2025

Accepted: 08 January 2025

Keywords:

connectome; functional connectivity; heterogeneity; neurotransmitter; structural covariance


Corresponding authors:

Wenzhou Zhang and Shaoqiang Han;

Emails: hnzzwz@hotmail.com;

shaoqianghan@163.com

Disrupted intersubject variability architecture in structural and functional brain connectomes in major depressive disorder

Keke Fang^{1,2,3}, Baohong Wen⁴, Liang Liu⁴, Shaoqiang Han⁴  and Wenzhou Zhang^{1,2,3}

¹Department of Pharmacy, The Affiliated Cancer Hospital of Zhengzhou University & Henan Cancer Hospital, Zhengzhou 450008, China; ²Henan Engineering Research Center for Tumor Precision Medicine and Comprehensive Evaluation, Henan Cancer Hospital; ³Henan Provincial Key Laboratory of Anticancer Drug Research, Henan Cancer Hospital and ⁴Department of Magnetic Resonance Imaging, The First Affiliated Hospital of Zhengzhou University, Henan Province, China

Abstract

Background. Major depressive disorder (MDD) is a heterogeneous condition characterized by significant intersubject variability in clinical presentations. Recent neuroimaging studies have indicated that MDD involves altered brain connectivity across widespread regions. However, the variability in abnormal connectivity among MDD patients remains understudied.

Methods. Utilizing a large, multi-site dataset comprising 1,276 patients with MDD and 1,104 matched healthy controls, this study aimed to investigate the intersubject variability of structural covariance (IVSC) and functional connectivity (IVFC) in MDD.

Results. Patients with MDD demonstrated higher IVSC in the precuneus and lingual gyrus, but lower IVSC in the medial frontal gyrus, calcarine, cuneus, and cerebellum anterior lobe. Conversely, they exhibited an overall increase in IVFC across almost the entire brain, including the middle frontal gyrus, anterior cingulate cortex, hippocampus, insula, striatum, and precuneus. Correlation and mediation analyses revealed that abnormal IVSC was positively correlated with gray matter atrophy and mediated the relationship between abnormal IVFC and gray matter atrophy. As the disease progressed, IVFC increased in the left striatum, insula, right lingual gyrus, posterior cingulate, and left calcarine. Pharmacotherapy significantly reduced IVFC in the right insula, superior temporal gyrus, and inferior parietal lobule. Furthermore, we found significant but distinct correlations between abnormal IVSC and IVFC and the distribution of neurotransmitter receptors, suggesting potential molecular underpinnings. Further analysis confirmed that abnormal patterns of IVSC and IVFC were reproducible and MDD specificity.

Conclusions. These results elucidate the heterogeneity of abnormal connectivity in MDD, underscoring the importance of addressing this heterogeneity in future research.

Introduction

Major depressive disorder (MDD) is a highly heterogeneous syndrome characterized by significant intersubject variability in symptom manifestations, clinical trajectories, etiologies, and treatment responses (Bondar, Caye, Chekroud, & Kieling, 2020; Drysdale, Grosenick, & Downar, 2017; Krishnan & Nestler, 2008; Nguyen, Harder, Xiong, Kowalec, & Hägg, 2022). This clinical heterogeneity complicates individualized diagnosis and treatment evaluations, and mechanism research in MDD. Neuroimaging studies have shown that MDD exhibits substantial intersubject variations in neuroimaging metrics, such as gray matter morphology (Chen et al., 2016). This high variability hampers the ability to reach consistent findings in MDD research. A critical reason for this inconsistency is the reliance on case-control designs that focus on group-level effects and overlook intersubject heterogeneity (Wolfers et al., 2018). To address this heterogeneity, many attempts have been made, such as subtype analysis based on symptomatology or neuroimaging phenotype and even inferring subject-level neuroimaging differences (Han et al., 2023a; Wen et al., 2022). However, as a brain connectome disorder, MDD is characterized by abnormal structural and functional connections among large-scale brain systems (Fornito, Zalesky, & Breakspear, 2015; Kaiser, Andrews-Hanna, Wager, & Pizzagalli, 2015). The distribution of intersubject variability in brain connectome remains largely understudied.

Brain function depends on effective structural and functional connectomes between distinct brain systems. Neuroimaging studies typically assess the brain connectome using techniques such as intrinsic functional connectivity and structural covariance (Alexander-Bloch, Giedd, & Bullmore, 2013; Fox & Raichle, 2007). In healthy individuals, brain connectome architecture exhibits considerable intersubject variability, distinguishing individuals from others and underlying differences in cognition and behavior (Finn et al., 2015; Smith et al., 2015). This variability is

© The Author(s), 2025. Published by Cambridge University Press. This is an Open Access article, distributed under the terms of the Creative Commons Attribution-NonCommercial-NoDerivatives licence (<http://creativecommons.org/licenses/by-nc-nd/4.0/>), which permits non-commercial re-use, distribution, and reproduction in any medium, provided that no alterations are made and the original article is properly cited. The written permission of Cambridge University Press must be obtained prior to any commercial use and/or adaptation of the article.



CAMBRIDGE
UNIVERSITY PRESS

modulated by genetic factors (Gao et al., 2014). In a healthy brain, connectome variability shows a specific distribution pattern, with higher variability in the heteromodal association cortex and lower variability in unimodal cortices (Finn et al., 2015; Smith et al., 2015). This pattern is consistent across adults (Mueller et al., 2013) and neonates (Gao et al., 2014; Stoecklein et al., 2020) and is influenced by neuropsychiatric disorders (Dumlu, Ademoglu, & Sun, 2020; Sun et al., 2021). For example, patients with schizophrenia demonstrate higher intersubject variability of functional connectome (IVFC) than healthy controls in bilateral sensorimotor, visual, auditory, and subcortical regions. Additionally, altered IVFC is associated with clinical heterogeneity (Sun et al., 2021; Zhang, Xu, Ma, Qian, & Zhu, 2024). In temporal lobe epilepsy, altered IVFC is linked to impairment in attention, memory, and executive functioning (Dumlu et al., 2020). These findings have potential implications for the understanding of clinical heterogeneity and individualized clinical decision-making in these disorders. To our knowledge, only three studies have investigated altered intersubject variability of brain connectome in MDD (Gai et al., 2024a; Hou et al., 2023; Sun et al., 2021). These studies have two main limitations: they use a single dataset with a small sample size, limiting statistical power and reproducibility, and they focus solely on functional connectome, neglecting the structural connectome.

In this study, we aimed to investigate intersubject variability of functional (IVFC) and structural covariance connectome (IVSC) using a large, multi-site dataset comprising 1,276 patients with MDD and 1,104 matched healthy controls (HCs). First, we identified abnormal patterns of IVSC and IVFC in patients with MDD. Next, we examined associations between these abnormal patterns and clinical features, such as age of onset, medicine status, and symptom severity. Additionally, we explored the potential molecular underpinnings of abnormal patterns of IVSC and IVFC. Finally, we conducted reproducibility analyses to evaluate the robustness and reproducibility of these abnormal patterns and performed disease specificity analysis to determine whether these patterns were specific to MDD compared with other psychiatric disorders.

Materials and methods

Imaging dataset and preprocessing

The MDD imaging datasets used in this study were sourced from the REST-meta-MDD consortium (<http://rfmri.org/REST-meta-MDD>) (Chen et al., 2022; Yan et al., 2019), which includes data from 25 research sites and comprises 1,276 patients diagnosed with MDD (age: 36.23 ± 21.38 years, females: 63.71%) and 1,104 HCs (age: 36.15 ± 24.55 years, females: 58.06%). Data collection for all research sites was approved by local research ethics committees. Patients were diagnosed by experienced psychiatrists based on DSM-IV criteria for MDD. The severity of symptoms in patients was assessed using the Hamilton Depression Rating Scale (HAM-D) (Hamilton, 1960). Among the patients with MDD, 538 were first-episode individuals, 282 were recurrent cases, 447 people were medication-naïve and 408 were treated. Further details about demographic and clinical characteristics, as well as image acquisition protocols are thoroughly described in previous studies (Chen et al., 2022; Yan et al., 2019).

Structural and functional MRI images were preprocessed using standard analysis protocols across sites to minimize analytic variations. The preprocessing steps of structural and functional MRI images are detailed elsewhere (Chen et al., 2022; Yan et al., 2019). In this study, we directly utilized the released gray matter volume

(GMV) maps obtained via voxel-based morphometry analysis (Ashburner, 2009) and extracted averaged time courses of each brain region defined in the Craddock 200 brain atlas from the REST-meta-MDD consortium (<http://rfmri.org/REST-meta-MDD>) (Craddock, James, Holtzheimer, Hu, & Mayberg, 2012). We used the time courses without global signal regression for the reason being its implication in the pathogenesis of mental disorders (Dong et al., 2023; Han et al., 2019; Yang et al., 2014).

Construction of structural covariance and functional network and harmonization

The construction of intra-individual structural covariance networks followed the methodology outlined in a previous study (Yun et al., 2020). The mean gray matter volumes (GMVs) of 200 brain regions, defined in the Craddock 200 brain atlas, were corrected for age, sex, and site effects (Craddock et al., 2012). The resulting residuals were transformed to Z-scores using mean and standard deviation (SD) values of each brain region calculated from healthy controls (Vuoksima et al., 2016). A measure of joint variation between 200 morphometric features, represented as edge weights (distributed between 0 and 1), was calculated to form the network (Yun, Jang, Kim, Jung, & Kwon, 2015). This procedure yielded a 200×200 structural covariance connectome matrix for each subject.

Functional networks were constructed by calculating pairwise Pearson's correlation coefficients between brain regions, with the resulting values transformed into Fisher's Z scores. This process produced a 200×200 functional connectome matrix for each subject.

To minimize the site effect introduced by differences in scanners and acquisition protocols, the ComBat method was independently performed in structural and functional connections (Johnson, Li, & Rabinovic, 2007). ComBat is a technique widely used in neuroimaging studies to remove unwanted site variation while preserving biological variability. This approach helps mitigate the impact of site differences on imaging metrics (Fortin et al., 2017).

Group differences in intersubject variability of the structural and functional connectome

The intersubject variability of the structural and functional connectome (IVSC/IVFC) was calculated to measure the inter-individual deviation of regional connection profiles for each group separately (Mueller, Wang, Fox, Yeo, & Liu, 2013). The IVSC/IVFC for region k in subject i was denoted as $V_{i,k}$ and was computed as follows:

$$V_{i,k} = 1 - \text{mean}(\text{corr}(C_{i,k}, C_{j,k})) \text{ for } j = 1, 2, \dots, n$$

For each subject i , we first calculated the Pearson's correlation coefficients between the connection profiles of region k ($C_{i,k}$, the k -th column of the connection matrix of subject i) and those of every other subject j ($C_{j,k}$). Then, $V_{i,k}$ was estimated by subtracting the averaged correlation coefficient from 1. A larger $V_{i,k}$ indicates a greater deviation of regional connection profiles from its own group.

A two-tailed two-sample t-test was performed to investigate the group differences in IVFC and IVSC, correcting for age, sex, and site. Statistical significance was set at $p < 0.05$ with Bonferroni correction for multiple comparisons. For the comparison of IVFC, mean framewise displacement (FD) was additionally corrected due to its significant effect on measures of functional connectivity (Circic et al., 2018).

Associations among distributions of IVSC, gray matter morphological atrophy, and abnormal patterns of regional structural covariance connectome

We investigated the relationships among distributions of IVSC, gray matter morphological atrophy, and abnormal patterns of regional structural covariance connectome. Specifically, we examined whether brain regions with more severe gray matter morphological atrophy exhibited higher intersubject variability or vice versa. Regional gray matter morphological atrophy (unthresholded t-static vector) was obtained by comparing harmonized regional GMVs between HCs and MDD with a two-sample t-test. Abnormal patterns of regional structural covariance connectome (unthresholded t-static vector) were obtained by comparing averaged intra-individual SCs between MDD and HCs using a two-sample t-test. We then calculated paired Spearman's correlation coefficients among these patterns.

Given the significant correlations between abnormal IVSC and gray matter atrophy, and between abnormal IVSC and IVFC (see results), we further hypothesized that IVSC mediates the relationship between gray matter atrophy and abnormal IVFC. To test this, we employed a standard three-variable mediation analysis using the Mediation Toolbox (<https://github.com/canlab/MediationToolbox>) (Wager, Davidson, Hughes, Lindquist, & Ochsner, 2008). More details about this model were described elsewhere (Wager et al., 2008). Mediation analysis assesses whether the relationship between two variables is explained by a third variable (the mediator). In this model, gray matter atrophy was the independent variable, IVFC was the dependent variable, and IVSC was the mediator. The significance of the mediation model was estimated using the bias-corrected bootstrap approach with 10,000 random samplings.

Associations between IVSC and IVFC and clinical features

To examine the impact of episodicity (first episode versus recurrent) and medication status (treated versus untreated) on the distributions of IVSC and IVFC, we conducted a two-sample t-test to compare subgroup differences. We also analyzed IVSC and IVFC differences between male and female patients, using a two-tailed two-sample t-test. Statistical significance was set at $p < 0.05$ with Bonferroni correction. Additionally, we computed Spearman's correlation between previously identified abnormal IVFC/IVSC and the total score of HAM-D.

Association between distributions of abnormal IVSC and IVFC and neurotransmitter receptors/transporters

Then, we examined the relationship between distributions of abnormal IVSC and IVFC and neurotransmitter receptors/transporters profiles to explore potential molecular underpinnings. Neurotransmitter receptors/transporters profiles were obtained from a PET-derived neurotransmitter receptors/transporters atlas (Hansen & Shafiei, 2022b), which includes serotonin (5HT_{1A}) (Savli et al., 2012), 5HT_{1B} (Baldassarri et al., 2018; Gallezot et al., 2010; Matuskey et al., 2014; Murrough et al., 2011; Murrough et al., 2011; Saricicek et al., 2015; Savli et al., 2012), 5HT_{2A} (Beliveau & Ganz, 2017, 5HT₄ (Beliveau & Ganz, 2017, 5HT₆ (Radhakrishnan et al., 2018; Radhakrishnan et al., 2020), 5HTT (Beliveau & Ganz, 2017), norepinephrine ($\alpha_4\beta_2$) (Baldassarri et al., 2018; Hillmer et al., 2016), M₁ (Naganawa et al., 2021), VACHT (Aghourian, Legault-Denis, Soucy, & Rosa-Neto, 2017; Bedard et al., 2019), cannabinoid (CB₁) (D'Souza et al., 2016; Neumeister et al., 2012; Normandin et al.,

2015; Ranganathan et al., 2016), dopamine (D₁) (Kaller et al., 2017), D₂ (Sandiego et al., 2015; Slifstein et al., 2015; Smith et al., 2019; Zakiniiez et al., 2019), DAT (Dukart et al., 2018), GABA (GABA_A) (Nørgaard et al., 2021), histamine (H₃) (Gallezot et al., 2017), glutamate (mGluR₅) (DuBois et al., 2016; Smart et al., 2019), NMDA (Galovic et al., 2021; McGinnity et al., 2014), opioid (MOR) (Kantonen et al., 2020), and norepinephrine (NET) (Belfort-DeAguiar et al., 2018; Ding et al., 2010; Li et al., 2014; Sanchez-Rangel et al., 2020). PET images were averaged within each study, normalized to the MNI-ICBM 152 non-linear 2009 template, parcellated into 200 brain regions, and Z-scored (Hansen & Shafiei, 2022a, b).

We constructed a multilinear model to assess the association between neurotransmitter receptors/transporters profiles and abnormal IVSC and IVFC patterns (unthresholded t-static vectors) separately. The significance of these multilinear models was evaluated through permutation testing (10000 times) with Bonferroni correction. To further understand the relative importance of each predictor (neurotransmitter receptor/transporter profile) in the model's overall predictive power, we conducted dominance analysis for each multilinear model. This analysis evaluates the impact of each predictor on the model fit by considering all possible combinations of predictors, resulting in $2^n - 1$ subset models for n predictors (Budescu, 1993). We used total dominance value to gauge each of the predictor's relative significance, calculated as the mean increase in explained variance (R^2) across all subset models in which it is included (Budescu, 1993).

Reproducibility and disease specificity analysis

To assess the robustness and reproducibility of abnormal IVSC and IVFC patterns, we performed several validation analyses. First, we validated these patterns using an alternative brain atlas, the Automated Anatomical Labeling (AAL) atlas, to ensure results were not dependent on the specific parcellation scheme used (Tzourio-Mazoyer et al., 2002). Second, we employed a split-sample method to evaluate whether abnormal IVSC and IVFC patterns were consistent across two halves of the dataset. We randomly divided patients into two subgroups, computed abnormal patterns (unthresholded t-statistic vectors) for each subgroup separately, and calculated Spearman's correlation coefficients to measure similarity. This process was repeated 100 times to minimize random selection errors. Third, we conducted leave-one-site-out validation to reduce the influence of specific sites. For each iteration, we excluded one site, computed abnormal IVSC and IVFC patterns using the remaining sites, and calculated Spearman's correlation coefficients between the new patterns and those from all sites.

Additionally, to investigate whether abnormal IVSC and IVFC patterns are specific to MDD, we compared these patterns with those in schizophrenia using another independent dataset sourced from the Centre for Biomedical Research Excellence (COBRE, http://fcon_1000.projects.nitrc.org/indi/retro/cobre.html) (Collin, Kahn, de Reus, Cahn, & van den Heuvel, 2014). The COBRE dataset includes 72 patients with schizophrenia and matched 74 HCs. Detailed information about the dataset and data acquisition protocols can be found elsewhere (Collin et al., 2014).

Results

Demographics and clinical characteristics

Demographics and clinical characteristics are detailed in Table 1.

Table 1. Demographic and clinical information of participants

	MDD (<i>n</i> = 1276)	HCs (<i>n</i> = 1104)	<i>p</i>
Age (year, mean \pm SD)	36.23 \pm 14.62	36.15 \pm 24.55	0.898 ^a
Gender (N female, %)	813 (63.71%)	641 (58.06%)	0.005 ^b
HAMD (mean \pm SD)	20.50 \pm 7.66	–	–
Illness duration (month, mean \pm SD)	36.46 \pm 59.68	–	–
Episodicity (N, %)			
First	538 (42.16%)	–	–
Recurrent	282 (22.10%)	–	–
Unknown	456 (35.74%)	–	–
Medication status (N, %)			
Untreated	447 (35.03%)	–	–
Treated	408 (31.97%)	–	–
Unknown	421 (32.99%)	–	–
Mean FD, mean \pm SD	0.14 \pm 0.01	0.13 \pm 0.01	0.863 ^a

Note: MDD, major depressive disorder; HCs, healthy controls; HAMD, Hamilton Depression Rating Scale; FD, framewise displacement.

^aTwo sample t test.

^bChi-square test.

Abnormal IVSC and IVFC patterns in MDD

Compared with HCs, patients with MDD demonstrated significantly higher IVSC in the precuneus and lingual gyrus but lower IVSC in the medial frontal gyrus, calcarine, cuneus, and cerebellum anterior lobe ($p < 0.05$ with Bonferroni correction). The abnormal pattern of IVSC is depicted in Figure 1 and Supplementary Table S1. Conversely, patients with MDD exhibited increased IVFC across nearly the entire brain ($p < 0.05$ with Bonferroni correction) including the middle frontal gyrus, anterior cingulate cortex, hippocampus, insula, striatum, and precuneus (Figure 1, Supplementary Table S1).

Additionally, the spatial distribution of abnormal IVSC pattern (un-thresholded t-static vector) was significantly correlated with the distribution of abnormal IVFC pattern (Spearman's $r = -0.21$, $p = 0.003$, see Figure 1).

More severe gray matter morphological atrophy is associated with higher IVSC

We observed significant spatial correlations between abnormal IVSC patterns and gray matter morphological atrophy, with a Spearman's correlation coefficient of $r = 0.22$ (Bonferroni corrected $p = 0.006$, see Figure 2a). There was also a strong correlation between abnormal IVSC pattern and the regional structural covariance connectome (Spearman's $r = 0.49$, Bonferroni corrected $p < 0.001$). Gray matter morphological atrophy showed a marginal correlation with an abnormal pattern of regional structural covariance connectome (Spearman's $r = 0.13$, uncorrected $p = 0.07$, see Figure 2b).

Additionally, mediation analysis result showed that IVSC mediated the effects of gray matter atrophy pathway on IVFC in MDD (total effect (path C) = -0.48 , 95% confidence interval (CI) = $[-0.93, -0.02]$, $p = 0.033$; direct effect (path C') = -0.34 , 95% CI = $[-0.56, -0.08]$, $p = 0.143$; indirect effect (path AB) = -0.15 , 95% CI = $[-0.35, -0.03]$, $p = 0.016$, Figure 2c).

Abnormal IVFC shows a close relationship with clinical features

No significant effects of episodicity (first episode versus recurrent) and medication status (treated versus untreated) were observed on

IVSC ($p > 0.05$ with Bonferroni correction). Similarly, there were no significant correlations between abnormal IVSC and the total score of HAMD ($p > 0.05$ with Bonferroni correction).

For IVFC, recurrent patients demonstrated significantly greater variability ($p < 0.05$ with Bonferroni correction) than first-episode patients in the left striatum, insula, right lingual gyrus, posterior cingulate, and left calcarine (Figure 3). Treated patients showed lower variability ($p < 0.05$ with Bonferroni correction) than untreated patients in the right insula, superior temporal gyrus, and inferior parietal lobule (Figure 3). No significant correlations between abnormal IVFC and the total score of HAMD were observed ($p > 0.05$ with Bonferroni correction).

There were no significant differences between male patients and female patients in either IVSC or IVFC ($p > 0.05$ with Bonferroni correction).

Association between abnormal IVSC/IVFC pattern and neurotransmitter receptors/transporters

We explored the associations between neurotransmitter receptors/transporters profiles and abnormal IVSC and IVFC patterns using multilinear models. The goodness-of-fit of these models (adjusted R^2) was 0.42 (F-statistic (200,180) = 8.68) for IVSC and 0.25 (F-statistic (200,180) = 4.39) for IVFC (see Figure 4a). Permutation testing confirmed that these models performed significantly better than chance, with permutation $p < 0.05$ after Bonferroni correction (see Figure 4b).

Dominance analysis identified key neurotransmitter receptors associated with each abnormal pattern. Specifically, MOR and CB₁ were significant for abnormal IVSC, while GABA_A was crucial for abnormal IVFC (see Figure 4c).

Reproducibility and disease specificity analysis

Reproducibility analysis confirmed the robustness and reproducibility of abnormal IVSC and IVFC patterns. Abnormal IVSC/IVFC patterns obtained using the AAL brain atlas were consistent with our main results. Patients with MDD demonstrated both increased

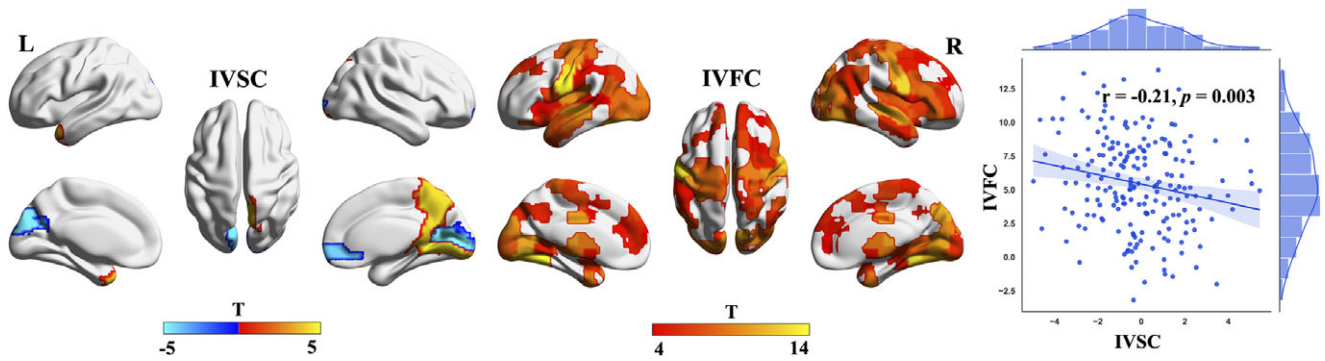


Figure 1. Abnormal patterns of intersubject variability of structural covariance (IVSC) and functional connectome (IVFC) in patients with MDD and the Spearman's correlation between them.

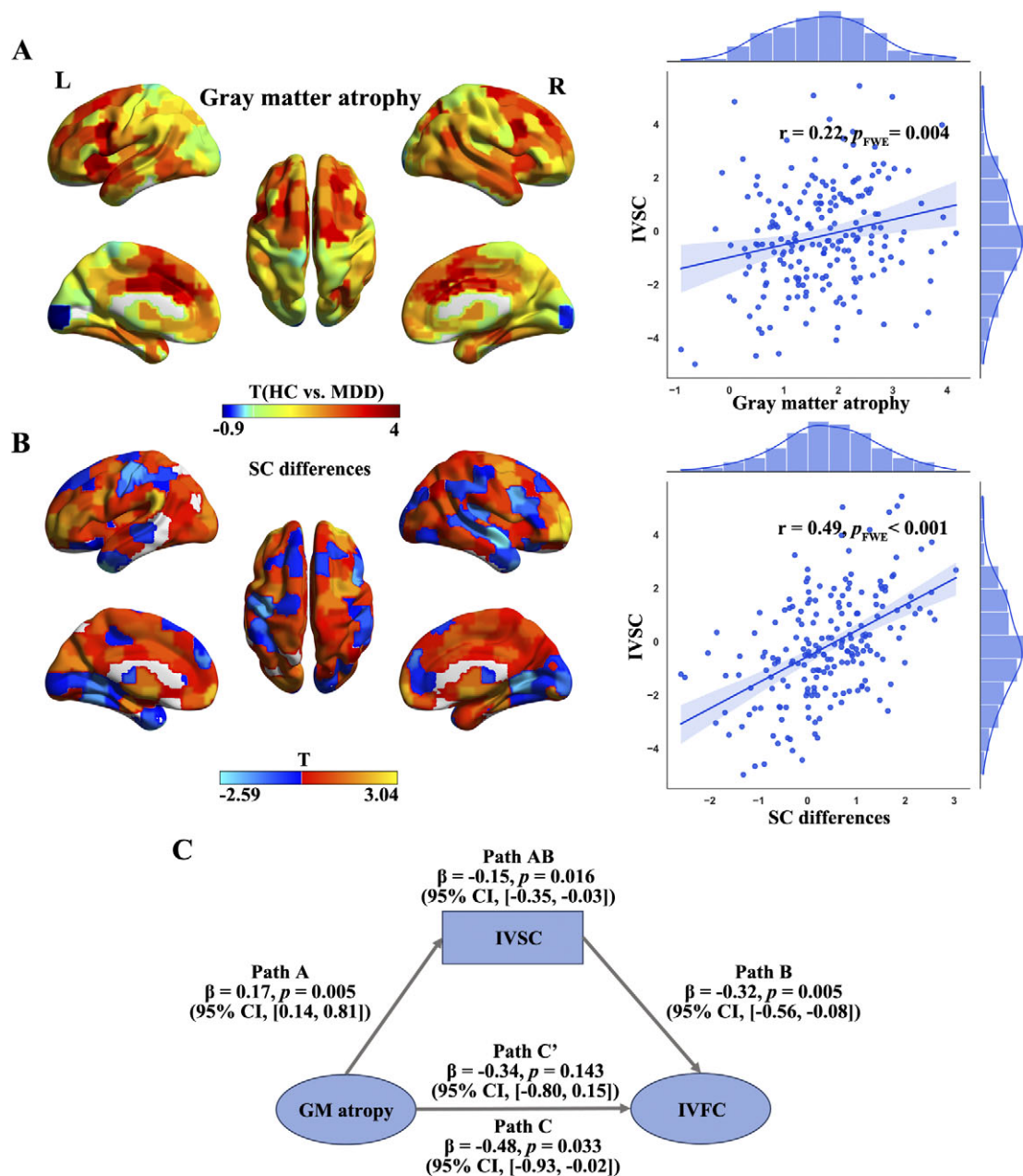


Figure 2. Associations between abnormal IVSC and gray matter morphological atrophy and abnormal patterns of regional structural covariance connectome (SC differences). (A). The distribution of gray matter morphological atrophy (t statistics of healthy controls vs. patients with MDD) and its Spearman's correlation with abnormal IVSC. (B). The distribution of SC differences and its Spearman's correlation with abnormal IVSC. (C). Abnormal IVSC has a mediating effect between gray matter atrophy and abnormal IVFC.

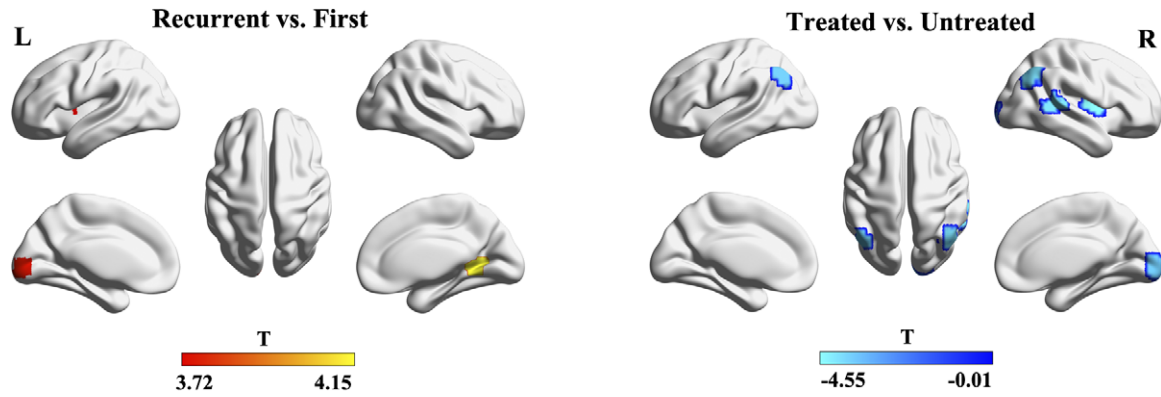


Figure 3. Group comparison results of IVFC between patient subgroups ($p < 0.05$ with Bonferroni correction).

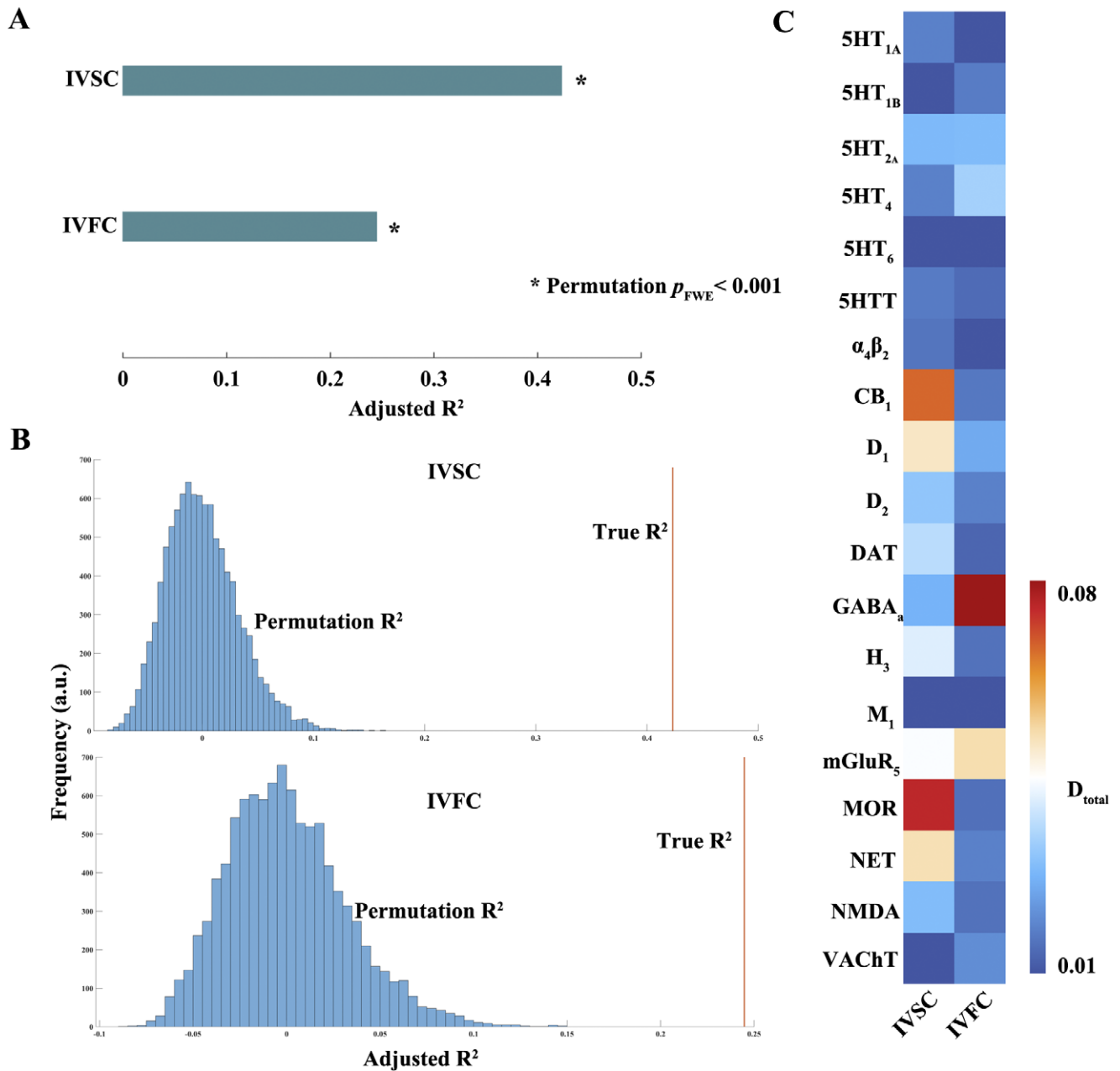


Figure 4. Associations between distributions of neurotransmitter receptors/transporters and abnormal IVSC and IVFC. (a). The goodness of fits (adjusted R^2) of multilinear models between distributions of neurotransmitter receptors/transporters and abnormal IVSC and IVFC. The significance is assessed through permutation testing. (b). Permutation testing results indicate that these performances of models (true R^2) are significantly better than chance (permutation R^2). (c). Dominance analysis is employed to determine the relative importance of predictors for each multilinear model. Total dominance values (d_{total}), indicative of the predictors' relative importance, are depicted.

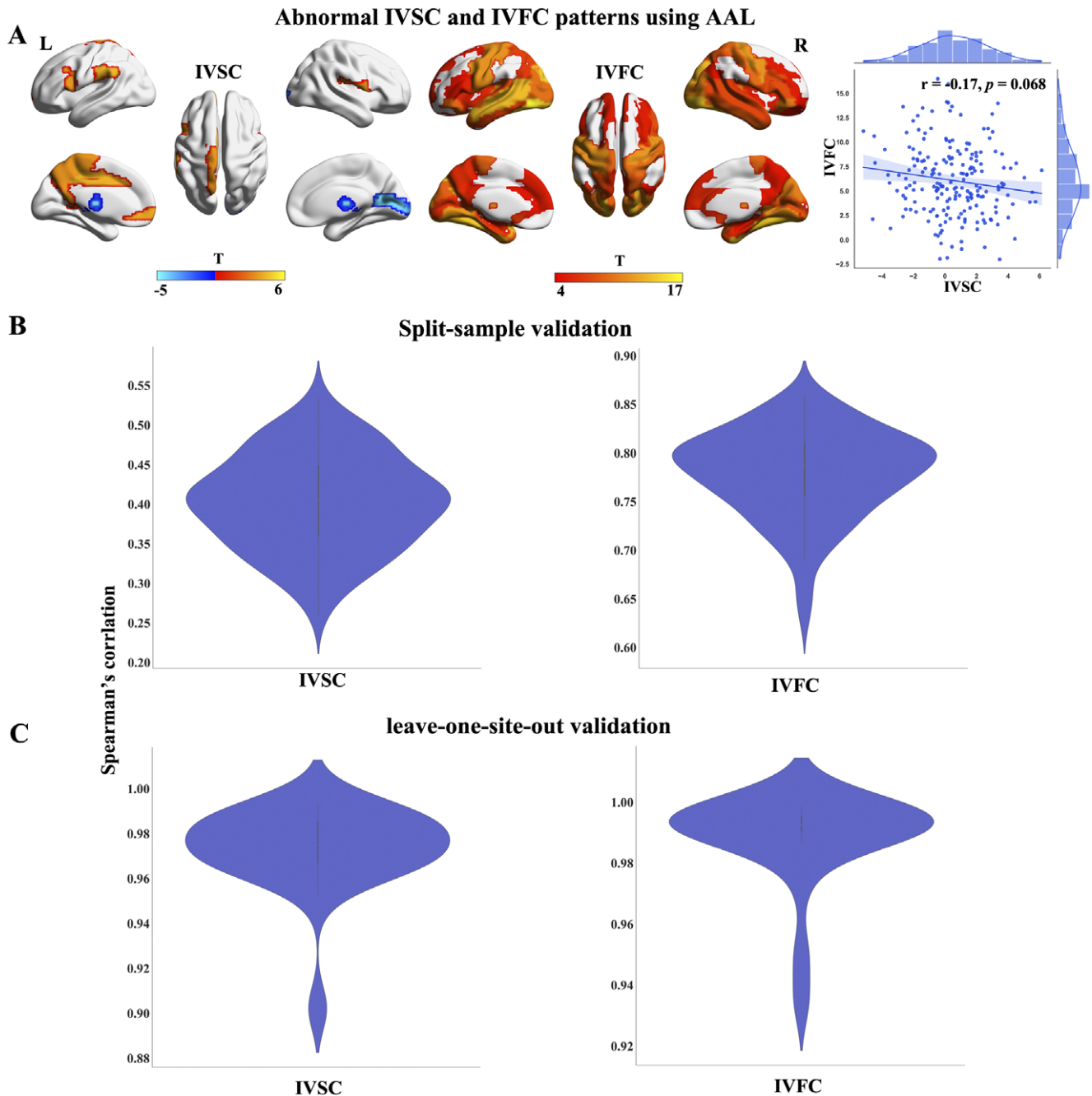


Figure 5. Reproducibility analysis results. (a). Abnormal patterns of IVSC and IVFC using AAL and Spearman's correlation between them. (b). The distribution of Spearman's correlations between randomly split halves (100 times). (c). Spearman's correlations between abnormal patterns of IVSC and IVFC using some study sites and those using all sites.

and decreased IVSC and overall increased IVFC compared to HCs (see Figure 5a). Additionally, abnormal IVSC patterns remained significantly positively correlated with gray matter atrophy using the AAL brain atlas (see Figure 5a). Second, abnormal IVSC and IVFC patterns showed strong reproducibility between randomly split halves, with mean (\pm SD) Spearman's correlations of 0.40 (± 0.06) for IVSC and 0.78 (± 0.05) for IVFC. The distributions of Spearman's correlations are shown in Figure 5b. Third, leave-one-site-out validation also supported the consistency of our results, with a mean (\pm SD) Spearman's correlations of 0.97 (± 0.19) for IVSC and 0.99 (± 0.15) for IVFC (see Figure 5c).

Finally, we investigated abnormal IVSC and IVFC patterns in schizophrenia using an independent dataset from COBRE. Patients

with schizophrenia demonstrated decreased IVSC and variable IVFC across brain regions compared to HCs (see Supplementary Figure S1). No significant association was found between abnormal IVSC and IVFC patterns in schizophrenia (Supplementary Figure S1). These results reinforced the MDD specificity of abnormal IVSC and IVFC patterns.

Discussion

This study represents the first systematic investigation of the heterogeneity in structural and functional connectomes in a large sample of patients with MDD. Our findings reveal that patients with MDD exhibit significantly higher IVSC in regions such as the

precuneus and calcarine while showing lower IVSC in the cuneus and medial frontal gyrus. Conversely, these patients demonstrate increased IVFC across a broad range of brain regions, including the middle frontal gyrus, anterior cingulate cortex, hippocampus, insula, striatum, and precuneus. Notably, the spatial distribution of abnormal IVSC patterns was negatively correlated with that of abnormal IVFC patterns. Higher IVSC was associated with more severe gray matter morphological atrophy, suggesting that structural covariance connectome abnormalities might be compensatory in response to gray matter loss. Our study also highlights that abnormal IVSC and IVFC patterns are associated with distinct neurotransmitter receptor distributions, indicating different molecular underpinnings. Specifically, MOR and CB1 were linked to abnormal IVSC, while GABA_A was associated with abnormal IVFC. This suggests that the variations in these neurotransmitter systems may contribute to the observed neuroimaging heterogeneity in MDD. Additionally, our findings underscore the disease-specific nature and reproducibility of these abnormal patterns, which were confirmed through various validation methods. Together, these findings provide systematic insights into the heterogeneity of structural and functional connectomes, underlying observed inconsistent dysconnectivity findings in previous studies and underline the need for addressing the heterogeneity of abnormal structural and functional connectomes to guide individualized clinical diagnosis and treatment evaluations.

In line with the diverse clinical manifestations of psychiatric disorders, neuroimaging studies have consistently observed higher intersubject variability of neuroimaging metrics among psychiatric patients. For instance, patients with schizophrenia demonstrate higher gray matter morphological variations and IVFC compared to healthy controls (Cheng *et al.*, 2025; Fang, Wen, Niu, Wan, & Zhang, 2022; Mo *et al.*, 2024; Sun *et al.*, 2021). Similarly, previous studies have reported elevated intersubject variability of multi-modal connectomes in MDD (Gai *et al.*, 2024b; Han *et al.*, 2023; Hou *et al.*, 2023). However, these studies have some limitations such as small sample sizes and a focus on single-modal connectomes. Our study, leveraging a large multi-site dataset, represents a significant advancement by systematically investigating abnormal IVSC and IVFC in MDD. Our findings reveal that patients with MDD exhibited higher IVSC in the precuneus and lingual gyrus while showing lower IVSC in the medial frontal gyrus, calcarine, cuneus, and cerebellum anterior lobe. These structural and functional abnormalities are implicated in the pathology of MDD and correlate with diverse clinical manifestations (Gentili *et al.*, 2009; Smith, Pang, Servatius, Jiao, & Beck, 2016; Zhou *et al.*, 2024). Higher IVSC offers insights into previously contradictory findings related to structural and connectome abnormalities in MDD (Han *et al.*, 2023b; Han, Zheng, Li, Zhou, *et al.*, 2023; Hu *et al.*, 2024; Wang *et al.*, 2024; Zeng *et al.*, 2015). Notably, we found that higher IVSC correlated positively with gray matter atrophy, suggesting that structural covariance abnormalities might compensate for gray matter loss. It is important to note that lower IVSC in regions such as the medial frontal gyrus does not imply lower intersubject variability in all neuroimaging metrics. For example, despite lower IVSC in the medial frontal gyrus, schizophrenia patients have been reported to exhibit higher intersubject gray matter variability in this region compared to healthy controls (Alnæs *et al.*, 2019; Brugger & Howes, 2017; Fang *et al.*, 2022).

On the functional side, patients with MDD show overall higher IVFC relative to healthy controls. This finding is consistent with a previous study identifying higher intersubject heterogeneity in functional connectome in MDD (Hou *et al.*, 2023). However, the

authors failed to find significant results using the AAL brain atlas due to the limited sample size (Hou *et al.*, 2023). The elevated IVFC in MDD provides an explanation for the inconsistencies observed in prior studies regarding functional connectivity, such as alterations in the default mode network (Javaheripour *et al.*, 2021; Scalabrini *et al.*, 2020; Yang *et al.*, 2021). The overall elevated IVFC in MDD highlights the need for strategies to address neuroimaging heterogeneity, such as subgroup or individualized analysis. Our mediation analysis indicates that abnormal IVSC mediates the relationship between gray matter atrophy and IVFC. Moreover, IVFC is significantly influenced by illness duration and antidepressant treatment, aligning with the progression of structural dysfunction and offering insights into the progressive nature of MDD (Han *et al.*, 2021; Han *et al.*, 2023; Morris *et al.*, 2019; Verduijn *et al.*, 2015; Wang *et al.*, 2023). Antidepressant treatment also reduces IVFC, consistent with the known effects of these medications on functional connectivity (Tassone, Nezhad, Demchenko, Rueda, & Bhat, 2024; Zhang *et al.*, 2024).

Our study further reveals that abnormal IVSC and IVFC patterns are associated with specific neurotransmitter receptor distributions. Neurotransmitter receptors, which play a crucial role in synaptic plasticity and neural communication, are implicated in the pathophysiology of MDD (Shine, 2019). Neurotransmitter dysfunction is thought to drive disorder-specific cortical abnormalities and cross-disorder similarities in psychiatry (Hansen & Shafiei, 2022a, b). The effectiveness of modern antipsychotic and antidepressant drugs depends on the selective manipulation of neurotransmitter function (Hansen & Shafiei, 2022a). This study found that neurotransmitter receptor/transporter distributions account for 42% and 25% of the variability in abnormal IVSC and IVFC, respectively. Dominance analysis highlights MOR and CB₁ as significant for abnormal IVSC, while GABA_A is crucial for abnormal IVFC. These receptors are involved in mood and reward regulation, with evidence suggesting dysregulation of the endogenous opioid system in depression (Jelen, Stone, Young, & Mehta, 2022). For instance, MOR knockout mice exhibit reduced food-anticipatory activity and diminished motivation (Kas *et al.*, 2004; Papaleo, Kieffer, Tabarin, & Contarino, 2007). Although the pathological mechanisms underlying brain connectome alterations in psychiatric disorders remain poorly understood, this study further supports the involvement of receptors in abnormal intersubject variability of brain connectome, providing a new insight into the molecular bias of neuroimaging heterogeneity in MDD.

Despite these insights, our study has limitations. First, the cross-sectional design does not capture changes in IVSC and IVFC over time. Longitudinal studies are needed to validate our findings regarding disease progression. Second, the clinical information available for patients was limited, which restricted our ability to explore potential associations between other clinical features and abnormal IVSC and IVFC patterns in MDD. Third, the influence of comorbidity on abnormal IVSC and IVFC remains unexplored. E.g. whether patients who have comorbidities with other mental disorders would have higher IVSC/IVFC should be investigated in the future.

In conclusion, our study provides a comprehensive analysis of intersubject heterogeneity in multi-modal brain connectomes in MDD using a large, multi-site dataset. We identify distinct patterns of abnormal IVSC and IVFC, with abnormal IVSC positively correlated with gray matter atrophy and mediating the association between gray matter atrophy and abnormal IVFC. The reproducibility and disease specificity of these patterns underscore their

relevance, while the association with neurotransmitter receptor distributions bridges neuroimaging heterogeneity and molecular mechanisms. These findings contribute to a deeper understanding of MDD and highlight the need for individualized approaches in clinical diagnosis and treatment.

Supplementary material. The supplementary material for this article can be found at <http://doi.org/10.1017/S0033291725000078>.

Acknowledgments. The authors thank everyone who participated in this research.

Funding statement. This research study was supported by the Natural Science Foundation of China (81601467, 81871327, 62106229, 62476252), the Medical science and technology research project of Henan province (201701011, SBGJ202102103, SBGJ202101013, SBGJ202302068, S20240045), China Postdoctoral Science Foundation (2022 M712890), and Medical science and technology research project of Henan province (LHGJ20230217).

Competing interest. All authors declared no conflict of interest.

References

- Aghourian, M., Legault-Denis, C., Soucy, J. P., & Rosa-Neto, P. (2017). Quantification of brain cholinergic denervation in Alzheimer's disease using PET imaging with [(18)F]-FEOBV. *Molecular Psychiatry*, **22**, 1531–1538.
- Alexander-Bloch, A., Giedd, J. N., & Bullmore, E. T. (2013). Imaging structural co-variance between human brain regions. *Nature Reviews Neuroscience*, **14**, 322–336.
- Alnaes, D., Kaufmann, T., van der Meer, D., Córdova-Palomera, A., Rokicki, J., Moberget, T., Bettella, F., Agartz, I., Barch, D. M., Bertolino, A., Brandt, C. L., Cervenka, S., Djurovic, S., Doan, N. T., Eisenacher, S., Fatouros-Bergman, H., Flyckt, L., Di Giorgio, A., Haaveit, B., Placeholder Text ... Karolinska Schizophrenia, P. (2019). Brain heterogeneity in schizophrenia and its association with polygenic risk. *JAMA Psychiatry*, **76**, 739–748.
- Ashburner, J. (2009). Computational anatomy with the SPM software. *Magnetic Resonance Imaging*, **27**, 1163–1174.
- Baldassarri, S. R., Hillmer, A. T., Anderson, J. M., Jatlow, P., Nabulsi, N., Labaree, D., Cosgrove, K. P., O'Malley, S. S., Eissenberg, T., Krishnan-Sarin, S., & Esterlis, I. (2018). Use of electronic cigarettes leads to significant beta2-nicotinic acetylcholine receptor occupancy: Evidence from a PET imaging study. *Nicotine & Tobacco Research*, **20**, 425–433.
- Bedard, M. A., Aghourian, M., Legault-Denis, C., Postuma, R. B., Soucy, J. P., Gagnon, J. F., Pelletier, A., & Montplaisir, J. (2019). Brain cholinergic alterations in idiopathic REM sleep behaviour disorder: A PET imaging study with (18)F-FEOBV. *Sleep Medicine*, **58**, 35–41.
- Belfort-DeAguiar, R., Gallezot, J. D., Hwang, J. J., Elshafie, A., Yeckel, C. W., Chan, O., Carson, R. E., Ding, Y. S., & Sherwin, R. S. (2018). Noradrenergic activity in the human brain: A mechanism supporting the defense against hypoglycemia. *The Journal of Clinical Endocrinology & Metabolism*, **103**, 2244–2252.
- Beliveau, V., & Ganz, M. (2017). A high-resolution in vivo atlas of the human brain's Serotonin System. *Journal of Neuroscience*, **37**, 120–128.
- Bondar, J., Caye, A., Chekroud, A. M., & Kieling, C. (2020). Symptom clusters in adolescent depression and differential response to treatment: A secondary analysis of the treatment for adolescents with depression study randomised trial. *Lancet Psychiatry*, **7**, 337–343.
- Brugger, S. P., & Howes, O. D. (2017). Heterogeneity and homogeneity of regional brain structure in schizophrenia a meta-analysis. *JAMA Psychiatry*, **74**, 1104–1111.
- Budescu, D. V. (1993). Dominance analysis : A new approach to the problem of relative importance of predictors in multiple regression. *Psychological Bulletin*, **114**, 542–551.
- Chen, X., Lu, B., Li, H.-X., Li, X.-Y., Wang, Y.-W., Castellanos, F. X., Cao, L.-P., Chen, N.-X., Chen, W., Cheng, Y.-Q., Cui, S.-X., Deng, Z.-Y., Fang, Y.-R., Gong, Q.-Y., Guo, W.-B., Hu, Z.-J.-Y., Kuang, L., Li, B.-J., Li, L., ... Yan, C.-G. (2022). The DIRECT consortium and the REST-meta-MDD project: Towards neuroimaging biomarkers of major depressive disorder. *Psychoradiology*, **2**, 32–42.
- Chen, Z., Peng, W., Sun, H., Kuang, W., Li, W., Jia, Z., & Gong, Q. (2016). High-field magnetic resonance imaging of structural alterations in first-episode, drug-naïve patients with major depressive disorder. *Translational Psychiatry*, **6**, e942.
- Cheng, Y., Cai, H., Liu, S., Yang, Y., Pan, S., Zhang, Y., Mo, F., Yu, Y., & Zhu, J. (2025). Brain network localization of gray matter atrophy and neurocognitive and social cognitive dysfunction in schizophrenia. *Biological Psychiatry*, **97**, 148–156.
- Ciric, R., Rosen, A. F. G., Erus, G., Cieslak, M., Adebimpe, A., Cook, P. A., Bassett, D. S., Davatzikos, C., Wolf, D. H., & Satterthwaite, T. D. (2018). Mitigating head motion artifact in functional connectivity MRI. *Nature Protocols*, **13**, 2801–2826.
- Collin, G., Kahn, R. S., de Reus, M. A., Cahn, W., & van den Heuvel, M. P. (2014). Impaired rich club connectivity in unaffected siblings of schizophrenia patients. *Schizophrenia Bulletin*, **40**, 438–448.
- Craddock, R. C., James, G. A., Holtzheimer, P. E., Hu, X. P. P., & Mayberg, H. S. (2012). A whole brain fMRI atlas generated via spatially constrained spectral clustering. *Human Brain Mapping*, **33**, 1914–1928.
- D'Souza, D. C., Cortes-Briones, J. A., Ranganathan, M., Thurnauer, H., Creatura, G., Surti, T., Planeta, B., Neumeister, A., Pittman, B., Normandin, M., Kapinos, M., Ropchan, J., Huang, Y., Carson, R. E., & Skosnik, P. D. (2016). Rapid changes in CB1 receptor availability in cannabis dependent males after abstinence from Cannabis. *Biological Psychiatry: Cognitive Neuroscience and Neuroimaging*, **1**, 60–67.
- Ding, Y. S., Singhal, T., Planeta-Wilson, B., Gallezot, J. D., Nabulsi, N., Labaree, D., Ropchan, J., Henry, S., Williams, W., Carson, R. E., Neumeister, A., & Malison, R. T. (2010). PET imaging of the effects of age and cocaine on the norepinephrine transporter in the human brain using (S,S)-[(11)C]O-methylreboxetine and HRRT. *Synapse*, **64**, 30–38.
- Dong, D., Wang, Y., Zhou, F., Chang, X., Qiu, J., Feng, T., He, Q., Lei, X., & Chen, H. (2023). Functional connectome hierarchy in schizotypy and its associations with expression of schizophrenia-related genes. *Schizophr Bull.* 2024 Dec 20;51(1):145–158. doi: 10.1093/schbul/sbad179. PMID: 38156676; PMCID: PMC11661955.
- Drysdale, A. T., Grosenick, L., & Downar, J. (2017). Resting-state connectivity biomarkers define neurophysiological subtypes of depression. *Nature Medicine*, **23**, 28–38.
- DuBois, J. M., Rousset, O. G., Rowley, J., Porras-Betancourt, M., Reader, A. J., Labbe, A., Massarweh, G., Soucy, J. P., Rosa-Neto, P., & Kobayashi, E. (2016). Characterization of age/sex and the regional distribution of mGluR5 availability in the healthy human brain measured by high-resolution [(11)C] ABP688 PET. *European Journal of Nuclear Medicine and Molecular Imaging*, **43**, 152–162.
- Dukart, J., Holiga, Š., Chatham, C., Hawkins, P., Forsyth, A., McMillan, R., Myers, J., Lingford-Hughes, A. R., Nutt, D. J., Merlo-Pich, E., Risterucci, C., Boak, L., Umbrecht, D., Schobel, S., Liu, T., Mehta, M. A., Zelaya, F. O., Williams, S. C., Brown, G., ... Sambataro, F. (2018). Cerebral blood flow predicts differential neurotransmitter activity. *Scientific Reports*, **8**, 4074.
- Dumlu, S. N., Ademoglu, A., & Sun, W. (2020). Investigation of functional variability and connectivity in temporal lobe epilepsy: A resting state fMRI study. *Neuroscience Letters*, **733**.
- Fang, K. K., Wen, B. H., Niu, L. J., Wan, B., & Zhang, W. Z. (2022). Higher brain structural heterogeneity in schizophrenia. *Frontiers in Psychiatry*, **13**.
- Finn, E. S., Shen, X. L., Scheinost, D., Rosenberg, M. D., Huang, J., Chun, M. M., Papademetris, X., & Constable, R. T. (2015). Functional connectome fingerprinting: Identifying individuals using patterns of brain connectivity. *Nature Neuroscience*, **18**, 1664–1671.
- Fornito, A., Zalesky, A., & Breakspear, M. (2015). The connectomics of brain disorders. *Nature Reviews Neuroscience*, **16**, 159–172.
- Fortin, J. P., Parker, D., Tunç, B., Watanabe, T., Elliott, M. A., Ruparel, K., Roalf, D. R., Satterthwaite, T. D., Gur, R. C., Gur, R. E., Schultz, R. T., Verma, R., & Shinohara, R. T. (2017). Harmonization of multi-site diffusion tensor imaging data. *Neuroimage*, **161**, 149–170.
- Fox, M. D., & Raichle, M. E. (2007). Spontaneous fluctuations in brain activity observed with functional magnetic resonance imaging. *Nature Reviews Neuroscience*, **8**, 700–711.

- Gai, Q., Chu, T., Li, Q., Guo, Y., Ma, H., Shi, Y., Che, K., Zhao, F., Dong, F., Li, Y., Xie, H., & Mao, N. (2024a). Altered intersubject functional variability of brain white-matter in major depressive disorder and its association with gene expression profiles. *Human Brain Mapping*, **45**, e26670.
- Gai, Q., Chu, T. P., Li, Q. H., Guo, Y. T., Ma, H., Shi, Y. H., Che, K. L., Zhao, F., Dong, F. H., Li, Y. A., Xie, H. Z., & Mao, N. (2024b). Altered intersubject functional variability of brain white-matter in major depressive disorder and its association with gene expression profiles. *Human Brain Mapping*, **45**.
- Gallezot, J. D., Nabulsi, N., Neumeister, A., Planeta-Wilson, B., Williams, W. A., Singhal, T., Kim, S., Maguire, R. P., McCarthy, T., Frost, J. J., Huang, Y., Ding, Y. S., & Carson, R. E. (2010). Kinetic modeling of the serotonin 5-HT_{1B} receptor radioligand [(11)C]P943 in humans. *Journal of Cerebral Blood Flow & Metabolism*, **30**, 196–210.
- Gallezot, J. D., Planeta, B., Nabulsi, N., Palumbo, D., Li, X., Liu, J., Rowinski, C., Chidsey, K., Labaree, D., Ropchan, J., Lin, S. F., Sawant-Basak, A., McCarthy, T. J., Schmidt, A. W., Huang, Y., & Carson, R. E. (2017). Determination of receptor occupancy in the presence of mass dose: [(11)C]GSK189254 PET imaging of histamine H(3) receptor occupancy by PF-03654746. *Journal of Cerebral Blood Flow & Metabolism* **37**, 1095–1107.
- Galovic, M., Erlandsson, K., Fryer, T. D., Hong, Y. T., Manavaki, R., Sari, H., Chetcuti, S., Thomas, B. A., Fisher, M., Sephton, S., Canales, R., Russell, J. J., Sander, K., Årstad, E., Aigbirhio, F. I., Groves, A. M., Duncan, J. S., Thielemans, K., Placeholder TextPlaceholder Text ... Koepp, M. J. (2021). Validation of a combined image derived input function and venous sampling approach for the quantification of [(18)F]GE-179 PET binding in the brain. *Neuroimage*, **237**, 118194.
- Gao, W., Elton, A., Zhu, H. T., Alcauter, S., Smith, J. K., Gilmore, J. H., & Lin, W. L. (2014). Intersubject variability of and genetic effects on the brain's functional connectivity during infancy. *Journal of Neuroscience*, **34**, 11288–11296.
- Gentili, C., Ricciardi, E., Gobbi, M. I., Santarelli, M. F., Haxby, J. V., Pietrini, P., & Guazzelli, M. (2009). Beyond amygdala: Default Mode Network activity differs between patients with Social Phobia and healthy controls. *Brain Research Bulletin*, **79**, 409–413.
- Hamilton, M. (1960). A rating scale for depression. *Journal of Neurology, Neurosurgery and Psychiatry*, **23**, 56–62.
- Han, S., Cui, Q., Zheng, R., Li, S., Zhou, B., Fang, K., Sheng, W., Wen, B., Liu, L., Wei, Y., Chen, H., Chen, Y., Cheng, J., & Zhang, Y. (2023a). Parsing altered gray matter morphology of depression using a framework integrating the normative model and non-negative matrix factorization. *Nature Communications*, **14**, 4053.
- Han, S., Wang, X., He, Z., Sheng, W., Zou, Q., Li, L., Yang, Y., Guo, X., Fan, Y. S., Guo, J., Lu, F., Cui, Q., & Chen, H. (2019). Decreased static and increased dynamic global signal topography in major depressive disorder. *Progress in Neuro-Psychopharmacology & Biological Psychiatry*, **94**, 109665.
- Han, S., Zheng, R., Li, S., Liu, L., Wang, C., Jiang, Y., Wen, M., Zhou, B., Wei, Y., Pang, J., Li, H., Zhang, Y., Chen, Y., & Cheng, J. (2021). Progressive brain structural abnormality in depression assessed with MR imaging by using causal network analysis. *Psychol Med*. 2023 Apr; **53**(5):2146–2155. doi: 10.1017/S0033291721003986. Epub 2021 Sep 29. PMID: 34583785.
- Han, S. Q., Cui, Q., Zheng, R. P., Li, S. Y., Zhou, B. Q., Fang, K. K., Sheng, W., Wen, B. H., Liu, L., Wei, Y. R., Chen, H. F., Chen, Y., Cheng, J. L., & Zhang, Y. (2023b). Parsing altered gray matter morphology of depression using a framework integrating the normative model and non-negative matrix factorization. *Nature Communications*, **14**.
- Han, S. Q., Zheng, R. P., Li, S. Y., Liu, L., Wang, C. H., Jiang, Y., Wen, M. M., Zhou, B. Q., Wei, Y. R., Pang, J. Y., Li, H. F., Zhang, Y., Chen, Y., & Cheng, J. L. (2023). Progressive brain structural abnormality in depression assessed with MR imaging by using causal network analysis. *Psychological Medicine*, **53**, 2146–2155.
- Han, S. Q., Zheng, R. P., Li, S. Y., Zhou, B. Q., Jiang, Y., Fang, K. K., Wei, Y. R., Pang, J. Y., Li, H. F., Zhang, Y., Chen, Y., & Cheng, J. L. (2023). Resolving heterogeneity in depression using individualized structural covariance network analysis. *Psychological Medicine*, **53**, 5312–5321.
- Hansen, J. Y., & Shafiei, G. (2022a). Local molecular and global connectomic contributions to cross-disorder cortical abnormalities. *Nature Communications*, **13**, 4682.
- Hansen, J. Y., & Shafiei, G. (2022b). Mapping neurotransmitter systems to the structural and functional organization of the human neocortex. *Nature Neuroscience*, **25**, 1569–1581.
- Hillmer, A. T., Esterlis, I., Gallezot, J. D., Bois, F., Zheng, M. Q., Nabulsi, N., Lin, S. F., Papke, R. L., Huang, Y., Sabri, O., Carson, R. E., & Cosgrove, K. P. (2016). Imaging of cerebral $\alpha 4\beta 2^*$ nicotinic acetylcholine receptors with (–)-[(18)F]flubatine PET: Implementation of bolus plus constant infusion and sensitivity to acetylcholine in human brain. *Neuroimage*, **141**, 71–80.
- Hou, Z. L., Jiang, W. H., Li, F., Liu, X. Y., Hou, Z. H., Yin, Y. Y., Zhang, H. S., Zhang, H. X., Xie, C. M., Zhang, Z. J., Kong, Y. Y., & Yuan, Y. G. (2023). Linking individual variability in functional brain connectivity to polygenic risk in major depressive disorder. *Journal of Affective Disorders*, **329**, 55–63.
- Hu, X., Cheng, B. C., Tang, Y. Y., Long, T., Huang, Y., Li, P., Song, Y., Song, X. Y., Li, K., Yin, Y. J., & Chen, X. J. (2024). Gray matter volume and corresponding covariance connectivity are biomarkers for major depressive disorder. *Brain Research*, **1837**.
- Javaheripour, N., Li, M., Chand, T., Krug, A., Kircher, T., Dannlowski, U., Nenadic, I., Hamilton, J. P., Sacchet, M. D., Gotlib, I. H., Walter, H., Frodl, T., Grimm, S., Harrison, B., Wolf, C. R., Olbrich, S., van Wingen, G., Pezawas, L., Parker, G., ... Wagner, G. (2021). Altered resting-state functional connectome in major depressive disorder: A mega-analysis from the PsyMRI consortium. *Translational Psychiatry*, **11**.
- Jelen, L. A., Stone, J. M., Young, A. H., & Mehta, M. A. (2022). The opioid system in depression. *Neuroscience and Biobehavioral Reviews*, **140**.
- Johnson, W. E., Li, C., & Rabinovic, A. (2007). Adjusting batch effects in microarray expression data using empirical Bayes methods. *Biostatistics*, **8**, 118–127.
- Kaiser, R. H., Andrews-Hanna, J. R., Wager, T. D., & Pizzagalli, D. A. (2015). Large-scale network dysfunction in major depressive disorder: A meta-analysis of resting-state functional connectivity. *JAMA Psychiatry*, **72**, 603–611.
- Kaller, S., Rullmann, M., Patt, M., Becker, G. A., Luthardt, J., Girhardt, J., Meyer, P. M., Werner, P., Barthel, H., Bresch, A., Fritz, T. H., Hesse, S., & Sabri, O. (2017). Test-retest measurements of dopamine D(1)-type receptors using simultaneous PET/MRI imaging. *European Journal of Nuclear Medicine and Molecular Imaging*, **44**, 1025–1032.
- Kantonen, T., Karjalainen, T., Isojärvi, J., Nuutila, P., Tuisku, J., Rinne, J., Hietala, J., Kaasinen, V., Kallioikoski, K., Scheinin, H., Hirvonen, J., Vehtari, A., & Nummenmaa, L. (2020). Interindividual variability and lateralization of μ -opioid receptors in the human brain. *Neuroimage*, **217**, 116922.
- Kas, M. J. H., van den Bos, R., Baars, A. M., Lubbers, M., Lesscher, H. M. B., Hillebrand, J. J. G., Schuller, A. G., Pintar, J. E., & Spruijt, B. M. (2004). Mu-opioid receptor knockout mice show diminished food-anticipatory activity. *European Journal of Neuroscience*, **20**, 1624–1632.
- Krishnan, V., & Nestler, E. J. (2008). The molecular neurobiology of depression. *Nature*, **455**, 894–902.
- Li, C. S., Potenza, M. N., Lee, D. E., Planeta, B., Gallezot, J. D., Labaree, D., Henry, S., Nabulsi, N., Sinha, R., Ding, Y. S., Carson, R. E., & Neumeister, A. (2014). Decreased norepinephrine transporter availability in obesity: Positron Emission Tomography imaging with (S,S)-[(11)C]O-methylreboxetine. *Neuroimage*, **86**, 306–310.
- Matuskey, D., Bhagwagar, Z., Planeta, B., Pittman, B., Gallezot, J. D., Chen, J., Wanyiri, J., Najafzadeh, S., Ropchan, J., Geha, P., Huang, Y., Potenza, M. N., Neumeister, A., Carson, R. E., & Malison, R. T. (2014). Reductions in brain 5-HT_{1B} receptor availability in primarily cocaine-dependent humans. *Biological Psychiatry*, **76**, 816–822.
- McGinnity, C. J., Hammers, A., Riaño Barros, D. A., Luthra, S. K., Jones, P. A., Trigg, W., Micallef, C., Symms, M. R., Brooks, D. J., Koepp, M. J., & Duncan, J. S. (2014). Initial evaluation of 18F-GE-179, a putative PET Tracer for activated N-methyl D-aspartate receptors. *Journal of Nuclear Medicine* **55**, 423–430.
- Mo, F., Zhao, H., Li, Y., Cai, H., Song, Y., Wang, R., Yu, Y., & Zhu, J. (2024). Network localization of state and trait of auditory verbal hallucinations in schizophrenia. *Schizophrenia Bulletin*, **50**, 1326–1336.
- Morris, G., Puri, B. K., Walker, A. J., Maes, M., Carvalho, A. F., Bortolasci, C. C., Walder, K., & Berk, M. (2019). Shared pathways for neuroprogression and somatoprogession in neuropsychiatric disorders. *Neuroscience & Biobehavioral Reviews*, **107**, 862–882.

- Mueller, S., Wang, D., Fox, M. D., Yeo, B. T. T., & Liu, H. J. N. (2013). Individual variability in functional connectivity architecture of the human brain. *Neuron*, **77**, 586–595.
- Mueller, S., Wang, D. H., Fox, M. D., Yeo, B. T. T., Sepulcre, J., Sabuncu, M. R., Shafee, R., Lu, J., & Liu, H. S. (2013). Individual variability in functional connectivity architecture of the human brain. *Neuron*, **77**, 586–595.
- Murrough, J. W., Czeremak, C., Henry, S., Nabulsi, N., Gallezot, J. D., Gueorguieva, R., Planeta-Wilson, B., Krystal, J. H., Neumaier, J. F., Huang, Y., Ding, Y. S., Carson, R. E., & Neumeister, A. (2011). The effect of early trauma exposure on serotonin type 1B receptor expression revealed by reduced selective radioligand binding. *Archives of General Psychiatry*, **68**, 892–900.
- Murrough, J. W., Henry, S., Hu, J., Gallezot, J. D., Planeta-Wilson, B., Neumaier, J. F., & Neumeister, A. (2011). Reduced ventral striatal/ventral pallidal serotonin 1B receptor binding potential in major depressive disorder. *Psychopharmacology (Berl)*, **213**, 547–553.
- Naganawa, M., Nabulsi, N., Henry, S., Matuskey, D., Lin, S. F., Sliker, L., Schwarz, A. J., Kant, N., Jesudason, C., Ruley, K., Navarro, A., Gao, H., Ropchan, J., Labaree, D., Carson, R. E., & Huang, Y. (2021). First-in-human assessment of (11)C-LSN3172176, an M1 muscarinic acetylcholine receptor PET radiotracer. *Journal of Nuclear Medicine*, **62**, 553–560.
- Neumeister, A., Normandin, M. D., Murrough, J. W., Henry, S., Bailey, C. R., Luckenbaugh, D. A., Tuit, K., Zheng, M. Q., Galatzer-Levy, I. R., Sinha, R., Carson, R. E., Potenza, M. N., & Huang, Y. (2012). Positron emission tomography shows elevated cannabinoid CB1 receptor binding in men with alcohol dependence. *Alcohol, Clinical and Experimental Research*, **36**, 2104–2109.
- Nguyen, T. D., Harder, A., Xiong, Y., Kowalec, K., & Hägg, S. (2022). Genetic heterogeneity and subtypes of major depression. *Molecular Psychiatry*, **27**, 1667–1675.
- Nørgaard, M., Beliveau, V., Ganz, M., Svarer, C., Pinborg, L. H., Keller, S. H., Jensen, P. S., Greve, D. N., & Knudsen, G. M. (2021). A high-resolution in vivo atlas of the human brain's benzodiazepine binding site of GABA(A) receptors. *Neuroimage*, **232**, 117878.
- Normandin, M. D., Zheng, M. Q., Lin, K. S., Mason, N. S., Lin, S. F., Ropchan, J., Labaree, D., Henry, S., Williams, W. A., Carson, R. E., Neumeister, A., & Huang, Y. (2015). Imaging the cannabinoid CB1 receptor in humans with [(11)C]OMAR: Assessment of kinetic analysis methods, test-retest reproducibility, and gender differences. *Journal of Cerebral Blood Flow & Metabolism*, **35**, 1313–1322.
- Papaleo, F., Kieffer, B. L., Tabarin, A., & Contarino, A. (2007). Decreased motivation to eat in μ -opioid receptor-deficient mice. *European Journal of Neuroscience*, **25**, 3398–3405.
- Radhakrishnan, R., Matuskey, D., Nabulsi, N., Gaiser, E., Gallezot, J. D., Henry, S., Planeta, B., Lin, S. F., Ropchan, J., Huang, Y., Carson, R. E., & D'Souza, D. C. (2020). In vivo 5-HT(6) and 5-HT(2A) receptor availability in antipsychotic treated schizophrenia patients vs. unmedicated healthy humans measured with [(11)C]GSK215083 PET. *Psychiatry Research: Neuroimaging*, **295**, 111007.
- Radhakrishnan, R., Nabulsi, N., Gaiser, E., Gallezot, J. D., Henry, S., Planeta, B., Lin, S. F., Ropchan, J., Williams, W., Morris, E., D'Souza, D. C., Huang, Y., Carson, R. E., & Matuskey, D. (2018). Age-Related Change in 5-HT(6) receptor availability in healthy male volunteers measured with (11)C-GSK215083 PET. *Journal of Nuclear Medicine*, **59**, 1445–1450.
- Ranganathan, M., Cortes-Briones, J., Radhakrishnan, R., Thurnauer, H., Planeta, B., Skosnik, P., Gao, H., Labaree, D., Neumeister, A., Pittman, B., Surti, T., Huang, Y., Carson, R. E., & D'Souza, D. C. (2016). Reduced brain cannabinoid receptor availability in schizophrenia. *Biological Psychiatry*, **79**, 997–1005.
- Sanchez-Rangel, E., Gallezot, J. D., Yeckel, C. W., Lam, W., Belfort-DeAguiar, R., Chen, M. K., Carson, R. E., Sherwin, R., & Hwang, J. J. (2020). Norepinephrine transporter availability in brown fat is reduced in obesity: A human PET study with [(11)C] MRB. *International Journal of Obesity*, **44**, 964–967.
- Sandiego, C. M., Gallezot, J. D., Lim, K., Ropchan, J., Lin, S. F., Gao, H., Morris, E. D., & Cosgrove, K. P. (2015). Reference region modeling approaches for amphetamine challenge studies with [(11)C]FLB 457 and PET. *Journal of Cerebral Blood Flow & Metabolism*, **35**, 623–629.
- Saricicek, A., Chen, J., Planeta, B., Ruf, B., Subramanyam, K., Maloney, K., Matuskey, D., Labaree, D., Deserno, L., Neumeister, A., Krystal, J. H., Gallezot, J. D., Huang, Y., Carson, R. E., & Bhagwagar, Z. (2015). Test-retest reliability of the novel 5-HT1B receptor PET radioligand [(11)C]P943. *European Journal of Nuclear Medicine and Molecular Imaging*, **42**, 468–477.
- Savli, M., Bauer, A., Mitterhauser, M., Ding, Y. S., Hahn, A., Kroll, T., Neumeister, A., Haeusler, D., Ungersboeck, J., Henry, S., Isfahani, S. A., Rattay, F., Wadsak, W., Kasper, S., & Lanzenberger, R. (2012). Normative database of the serotonergic system in healthy subjects using multi-tracer PET. *Neuroimage*, **63**, 447–459.
- Scalabrini, A., Vai, B., Poletti, S., Damiani, S., Mucci, C., Colombo, C., Zanardi, R., Benedetti, F., & Northoff, G. (2020). All roads lead to the default-mode network-global source of DMN abnormalities in major depressive disorder. *Neuropsychopharmacology*, **45**, 2058–2069.
- Shine, J. M. (2019). Neuromodulatory influences on integration and segregation in the brain. *Trends in Cognitive Sciences*, **23**, 572–583.
- Slifstein, M., van de Giessen, E., Van Snellenberg, J., Thompson, J. L., Narendran, R., Gil, R., Hackett, E., Girgis, R., Ojeil, N., Moore, H., D'Souza, D., Malison, R. T., Huang, Y., Lim, K., Nabulsi, N., Carson, R. E., Lieberman, J. A., & Abi-Dargham, A. (2015). Deficits in prefrontal cortical and extrastriatal dopamine release in schizophrenia: A positron emission tomographic functional magnetic resonance imaging study. *JAMA Psychiatry*, **72**, 316–324.
- Smart, K., Cox, S. M. L., Scala, S. G., Tippler, M., Jaworska, N., Boivin, M., Séguin, J. R., Benkelfat, C., & Leyton, M. (2019). Sex differences in [(11)C] ABP688 binding: A positron emission tomography study of mGlu5 receptors. *European Journal of Nuclear Medicine and Molecular Imaging*, **46**, 1179–1183.
- Smith, C. T., Crawford, J. L., Dang, L. C., Seaman, K. L., San Juan, M. D., Vijay, A., Katz, D. T., Matuskey, D., Cowan, R. L., Morris, E. D., Zald, D. H., & Samanez-Larkin, G. R. (2019). Partial-volume correction increases estimated dopamine D2-like receptor binding potential and reduces adult age differences. *Journal of Cerebral Blood Flow & Metabolism*, **39**, 822–833.
- Smith, I. M., Pang, K. C. H., Servatius, R. J., Jiao, X. L., & Beck, K. D. (2016). Paired-housing selectively facilitates within-session extinction of avoidance behavior, and increases c-Fos expression in the medial prefrontal cortex, in anxiety vulnerable Wistar-Kyoto rats. *Physiology & Behavior*, **164**, 198–206.
- Smith, S. M., Nichols, T. E., Vidaurre, D., Winkler, A. M., Behrens, T. E. J., Glasser, M. F., Ugurbil, K., Barch, D. M., Van Essen, D. C., & Miller, K. L. (2015). A positive-negative mode of population covariation links brain connectivity, demographics and behavior. *Nature Neuroscience*, **18**, 1565–1567.
- Stoecklein, S., Hilgendorff, A., Li, M. L., Forster, K., Flemmer, A. W., Galie, F., Wunderlich, S., Wang, D. H., Stein, S., Ehrhardt, H., Dietrich, O., Zou, Q. H., Zhou, S. Q., Ertl-Wagner, B., & Liu, H. S. (2020). Variable functional connectivity architecture of the preterm human brain: Impact of developmental cortical expansion and maturation. *Proceedings of the National Academy of Sciences of the United States of America*, **117**, 1201–1206.
- Sun, X. Y., Liu, J., Ma, Q., Duan, J., Wang, X. D., Xu, Y. H., Xu, Z. L., Xu, K., Wang, F., Tang, Y. Q., He, Y., & Xia, M. R. (2021). Disrupted intersubject variability architecture in functional connectomes in schizophrenia. *Schizophrenia Bulletin*, **47**, 837–848.
- Tassone, V. K., Nezhad, F. G., Demchenko, I., Rueda, A., & Bhat, V. (2024). Amygdala biomarkers of treatment response in major depressive disorder: An fMRI systematic review of SSRI antidepressants. *Psychiatry Research: Neuroimaging*, **338**.
- Tzourio-Mazoyer, N., Landeau, B., Papathanassiou, D., Crivello, F., Etard, O., Delcroix, N., Mazoyer, B., & Joliot, M. (2002). Automated anatomical labeling of activations in SPM using a macroscopic anatomical parcellation of the MNI MRI single-subject brain. *Neuroimage*, **15**, 273–289.
- Verduijn, J., Milaneschi, Y., Schoevers, R. A., van Hemert, A. M., Beekman, A. T., & Penninx, B. W. (2015). Pathophysiology of major depressive disorder: Mechanisms involved in etiology are not associated with clinical progression. *Translational Psychiatry*, **5**, e649.
- Vuoksimaa, E., Panizzon, M. S., Chen, C. H., Fiecas, M., Eyler, L. T., Fennema-Notestine, C., Hagler, D. J., Franz, C. E., Jak, A. J., Lyons, M. J., Neale, M. C., Rinker, D. A., Thompson, W. K., Tsuang, M. T., Dale, A. M., & Kremen, W. S. (2016).

- Is bigger always better? The importance of cortical configuration with respect to cognitive ability. *Neuroimage*, **129**, 356–366.
- Wager, T. D., Davidson, M. L., Hughes, B. L., Lindquist, M. A., & Ochsner, K. N. (2008). Prefrontal-subcortical pathways mediating successful emotion regulation. *Neuron*, **59**, 1037–1050.
- Wang, Y., Genon, S., Dong, D., Zhou, F., Li, C., Yu, D., Yuan, K., He, Q., Qiu, J., Feng, T., Chen, H., & Lei, X. (2023). Covariance patterns between sleep health domains and distributed intrinsic functional connectivity. *Nature Communications*, **14**, 7133.
- Wang, Y., Yang, J., Zhang, H., Dong, D., Yu, D., Yuan, K., & Lei, X. (2024). Altered morphometric similarity networks in insomnia disorder. *Brain Structure and Function*, **229**, 1433–1445.
- Wen, J. H., Fu, C. H. Y., Tosun, D., Veturi, Y., Yang, Z. J., Abdulkadir, A., Mamourian, E., Srinivasan, D., Skampardon, I., Singh, A., Nawani, H., Bao, J. X., Erus, G., Shou, H. C., Habes, M., Doshi, J., Varol, E., Mackin, R. S., Sotiras, A., ..., ADNI, BIOCARD & BLSA (2022). Characterizing heterogeneity in neuroimaging, cognition, clinical symptoms, and genetics among patients with late-life depression. *JAMA Psychiatry*, **79**, 464–474.
- Wolfers, T., Doan, N. T., Kaufmann, T., Alnæs, D., Moberget, T., Agartz, I., Buitelaar, J. K., Ueland, T., Melle, I., Franke, B., Andreassen, O. A., Beckmann, C. F., Westlye, L. T., & Marquand, A. F. (2018). Mapping the heterogeneous phenotype of schizophrenia and bipolar disorder using normative models. *JAMA Psychiatry*, **75**, 1146–1155.
- Yan, C. G., Chen, X., Li, L., Castellanos, F. X., Bai, T. J., Bo, Q. J., Cao, J., Chen, G. M., Chen, N. X., Chen, W., Cheng, C., Cheng, Y. Q., Cui, X. L., Duan, J., Fang, Y. R., Gong, Q. Y., Guo, W. B., Hou, Z. H., Hu, L., ... Wang, C. Y. (2019). Reduced default mode network functional connectivity in patients with recurrent major depressive disorder. *Proceedings of the National Academy of Sciences of the United States of America*, **116**, 9078–9083.
- Yang, G. J., Murray, J. D., Repovs, G., Cole, M. W., Savic, A., Glasser, M. F., Pittenger, C., Krystal, J. H., Wang, X. J., Pearlson, G. D., Glahn, D. C., & Anticevic, A. (2014). Altered global brain signal in schizophrenia. *Proceedings of the National Academy of Sciences of the United States of America*, **111**, 7438–7443.
- Yang, H., Chen, X., Chen, Z. B., Li, L., Li, X. Y., Castellanos, F. X., Bai, T. J., Bo, Q. J., Cao, J., Chang, Z. K., Chen, G. M., Chen, N. X., Chen, W., Cheng, C., Cheng, Y. Q., Cui, X. L., Duan, J., Fang, Y. R., Gong, Q. Y., ... Yan, C. G. (2021). Disrupted intrinsic functional brain topology in patients with major depressive disorder. *Molecular Psychiatry*, **26**, 7363–7371.
- Yun, J. Y., Boedhoe, P. S. W., Vriend, C., Jahanshad, N., Abe, Y., Ameis, S. H., Anticevic, A., Arnold, P. D., Batistuzzo, M. C., Benedetti, F., Beucke, J. C., Bollettini, I., Bose, A., Brem, S., Calvo, A., Cheng, Y., Cho, K. I. K., Ciullo, V., Dallspezia, S., ... Kwon, J. S. (2020). Brain structural covariance networks in obsessive-compulsive disorder: A graph analysis from the ENIGMA Consortium. *Brain*, **143**, 684–700.
- Yun, J. Y., Jang, J. H., Kim, S. N., Jung, W. H., & Kwon, J. S. (2015). Neural correlates of response to pharmacotherapy in obsessive-compulsive disorder: Individualized cortical morphology-based structural covariance. *Progress in Neuro-Psychopharmacology & Biological Psychiatry*, **63**, 126–133.
- Zakariaeiz, Y., Hillmer, A. T., Matuskey, D., Nabulsi, N., Ropchan, J., Mazure, C. M., & Picciotto, M. R. (2019). Sex differences in amphetamine-induced dopamine release in the dorsolateral prefrontal cortex of tobacco smokers. *Neuropsychopharmacology*, **44**, 2205–2211.
- Zeng, L. L., Shen, H., Liu, L., Fang, P., Liu, Y. D., & Hu, D. W. (2015). State-dependent and trait-related gray matter changes in nonrefractory depression. *Neuroreport*, **26**, 57–65.
- Zhang, B., Rolls, E. T., Wang, X., Xie, C., Cheng, W., & Feng, J. F. (2024). Roles of the medial and lateral orbitofrontal cortex in major depression and its treatment. *Molecular Psychiatry*.
- Zhang, X., Xu, R., Ma, H., Qian, Y., & Zhu, J. (2024). Brain structural and functional damage network localization of suicide. *Biological Psychiatry*, **95**, 1091–1099.
- Zhou, E. Q., Wang, W., Ma, S. M., Xie, X. H., Kang, L. J., Xu, S. X., Deng, Z. P., Gong, Q., Nie, Z. W., Yao, L. H., Bu, L. H., Wang, F., & Liu, Z. C. (2024). Prediction of anxious depression using multimodal neuroimaging and machine learning. *Neuroimage*, **285**.